Electronic Supplementary Material (ESI) for Journal of Materials Chemistry C.

Supporting Information

Molecular understanding of π-conjugated polymer/solid-state ionic liquid complex as a highly sensitive and selective gas sensor

By Katherine Stewart,[a] Saurav Limbu,[a] James Nightingale,[a] Katia Pagano,[a] Byoungwook Park,[b] Soonil hong,[c] Kwanghee Lee,[b,c] Sooncheol Kwon[b] and Ji-Seon Kim*[a]*

[a]Department of Physics and Centre for Processable Electronics, Imperial College London, London, SW7 2AZ, United Kingdom
b. School of Materials Science and Engineering (SMSE), Gwangju Institute of Science and Technology (GIST), Gwangju 500-712, Republic of Korea
c. Research Institute for Solar and Sustainable Energies (RISE), Gwangju Institute of Science and Technology (GIST), Gwangju 500-712, Republic of Korea

*Correspondence to: kwansc@gist.ac.kr; ji-seon.kim@imperial.ac.uk

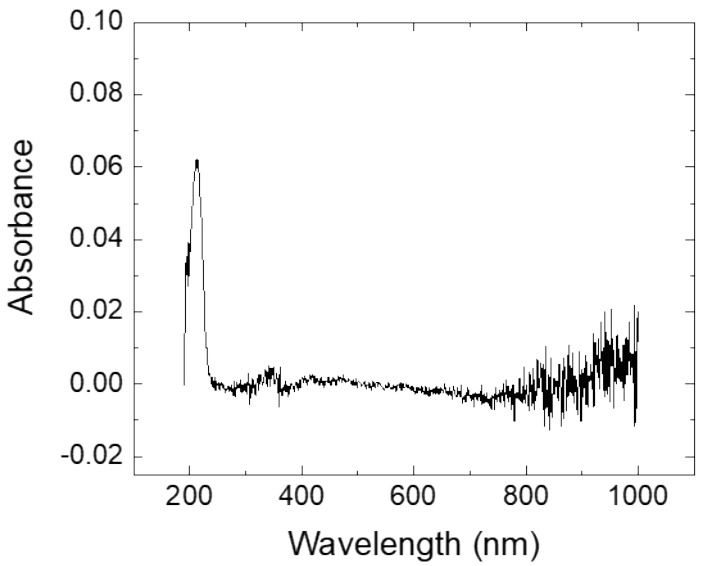

Fig. S1. Normalised absorbance spectra of neat [$C_1C_{12}IM^+$] [PF_6^-]

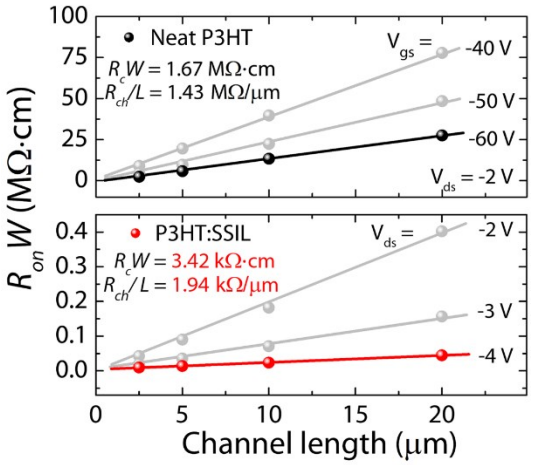

Figure S2. An evaluation of the contact and channel resistance of neat P3HT and P3HT:SSIL chemiresistors evaluated by a transfer line measurement (TLM).

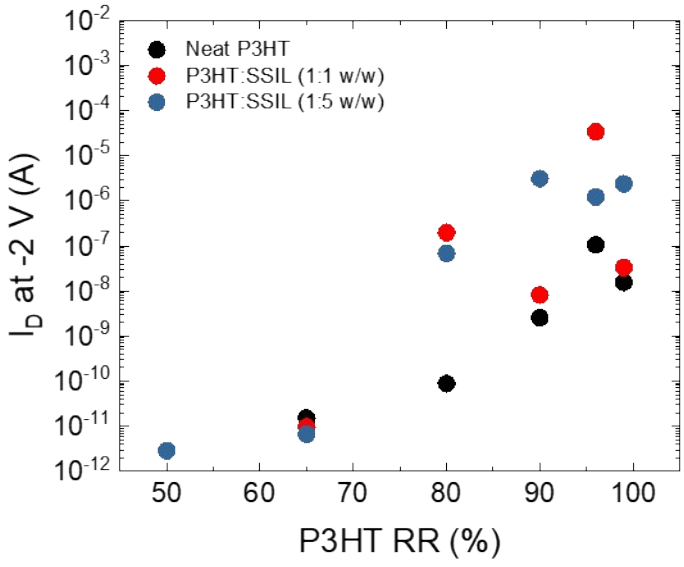

Fig. S3. c) Driven voltage dependence, mean drain current measured for each polymer under an applied bias of V_D = -2 V as a function of regioregulatiry.

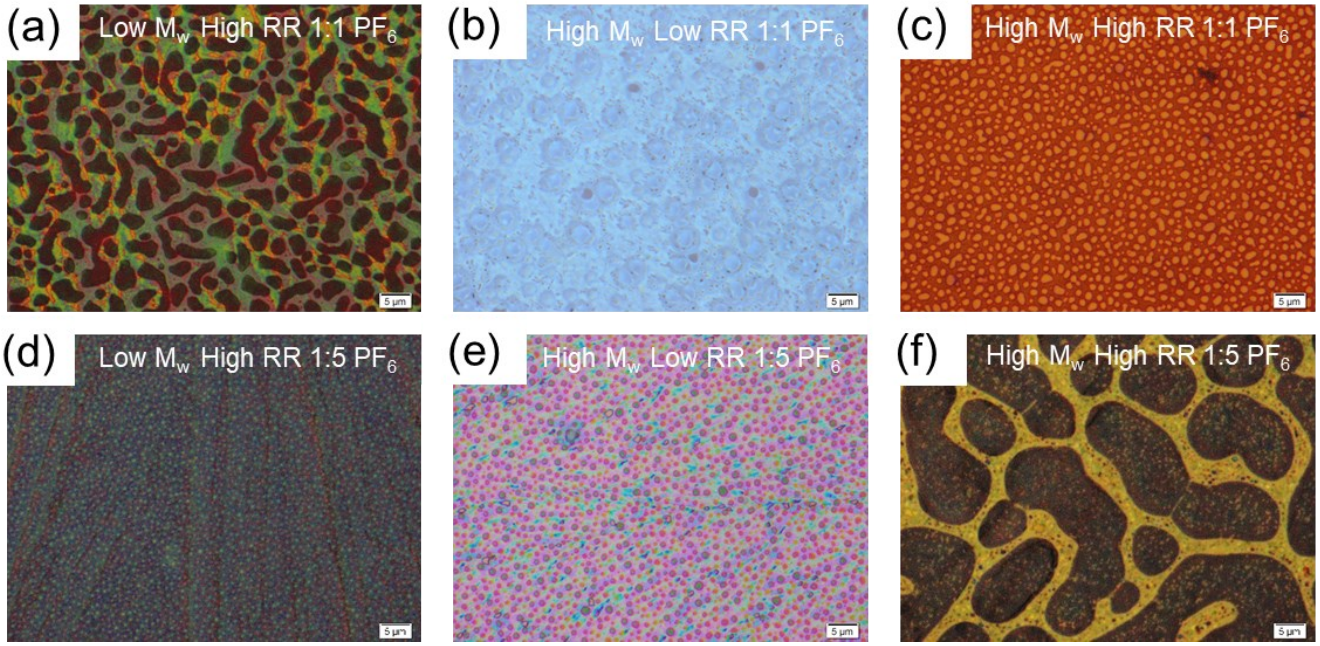

Fig. S4. Optical microscope images showing topography of P3HT blend thin films on quartz, scale bar 5µm. P3HT:SSIL 1:1 a) low M_w high RR, b) high M_w low RR and c) high M_w high RR and P3HT:SSIL 1:5 d) low M_w high RR, e) high M_w low RR and f) high M_w high RR P3HT.

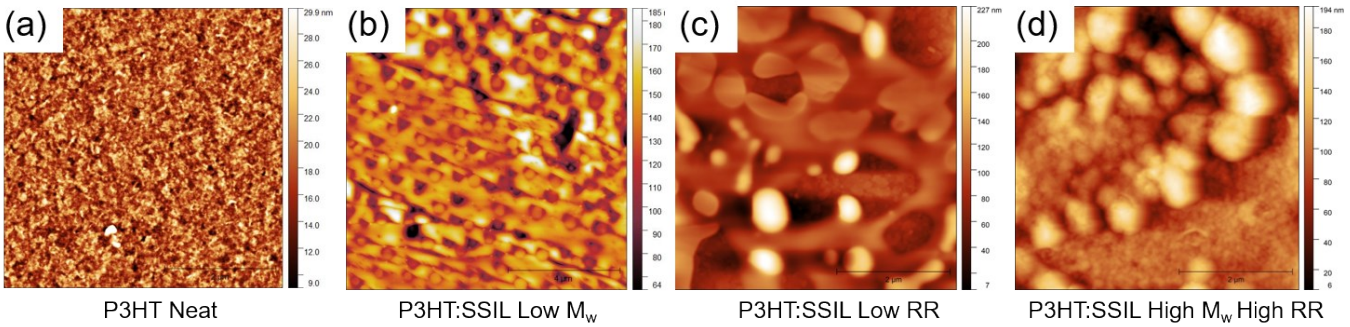

Fig. S5. Atomic force microscope images showing topography of P3HT blend thin films on quartz, scale bar 2µm for a) P3HT neat and P3HT:SSIL 1:1 b) low M_w high RR, c) high M_w low RR and d) high M_w high RR.

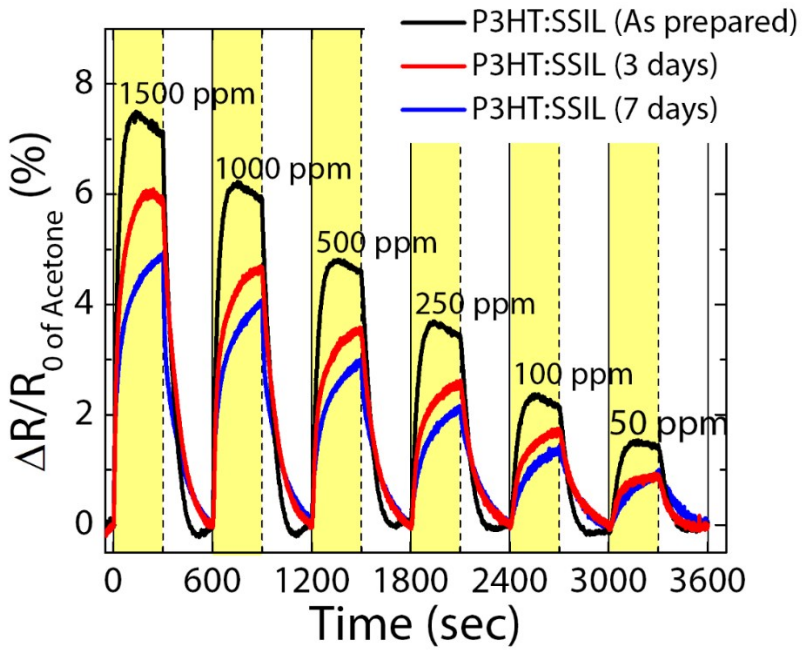

Figure S6. Stability test for P3HT:SSIL device that was stored in air and room temperature conditions for 7 days. The measurements were carried out at V_D = 2 V.

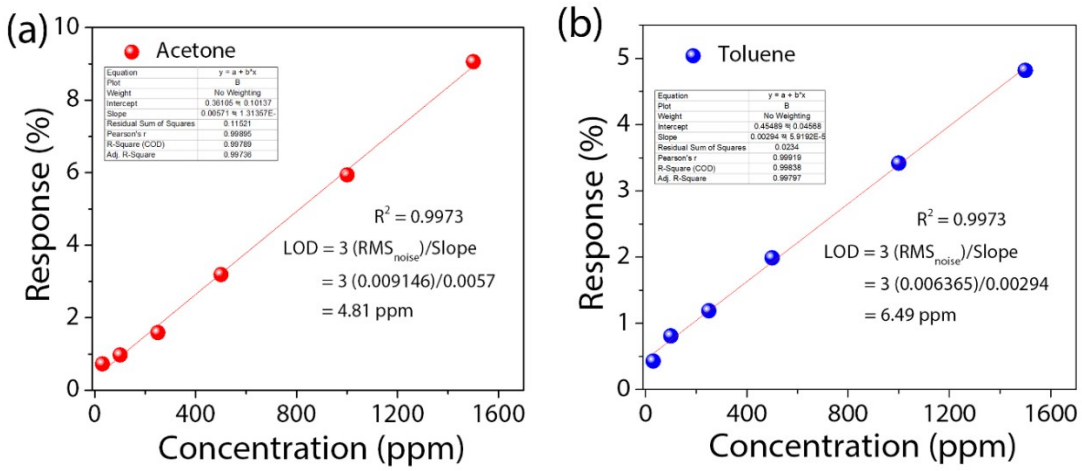

Figure S7. The limits of detection (LODs) of P3HT:SSIL chemiresistor for (a) acetone and (b) toluene exposure were calculated to be 4.81 ppm and 6.49 ppm, respectively, using the Inter-national Conference on Harmonization (ICH) model, in which the LOD is defined as 3 × (standard deviation/slope of regression line).[1,2]

Table S1. Comparison of Key Parameters of electrical acetone sensors using OCS as active layers.

Sensing Material	Sensor Type	Response definition †	Detect Limit	Sensitivity response	Reference
This work **P3HT:SSIL**	**Chemiresistor (2 terminal)**	**$\Delta R/R_0$**	**30 ppm**	**9% at 1500 ppm**	
P3HT	Chemiresistor (2 terminal)	ΔG/G	170 ppm	1.25% per 1ppm	[3]

PDDT-*ran*-PMT	Chemiresistor (2 terminal)	ΔG/G	170 ppm	-3.12% per 1ppm	[3]
PHT-*b*-PS	Chemiresistor (2 terminal)	ΔG/G	360 ppm	-0.76% per 1ppm	[3]
PHT-*b*-PMA	Chemiresistor (2 terminal)	ΔG/G	360 ppm	-1.45% per 1ppm	[3]
PHT-*b*-PBA	Chemiresistor (2 terminal)	ΔG/G	360 ppm	1.04% per 1ppm	[3]
P3HT	Chemiresistor (2 terminal)	$\Delta I_{DS}/I_{DS}$	680 ppm	$-1x10^{-6}$ per ppm	[4]
P3HT	Transistor (3 terminal)	$\Delta I_{DS}/I_{DS}$	3500 ppm	$-1x10^{-5}$ per ppm	[4]
DNTT	Transistor (3 terminal)	$\Delta I/I_0$	500 ppm	8% @ 500 ppm	[5]
DNTT-C_{10}	Transistor (3 terminal)	I/I_0	10 ppm	0.02 @10 pppm	[6]
DTBDT-C_6	Transistor (3 terminal)	I_{off}/I_{on}	>200 ppm	$2x10^0$ @ >200 ppm	[7]
PQT-12	Transistor (3 terminal)	$(I_{DS,gas}-I_{DS,air}-\Delta I_{ref})/I_{DS,air}$	16 200 ppm	10% at 16 200 ppm	[8]

† Response definition as given in source: ΔG/G = change in normalised conductance change, $\Delta I_{DS}/I_{DS}$, $\Delta I/I_0$ and I/I_0 = normalised source drain current response, I_{off}/I_{on} = ratio of drain-source current between gas on and gas off, $(I_{DS,gas}-I_{DS,air}-\Delta I_{ref})/I_{DS,air}$ = change in drain current where $I_{DS,gas}$ is the drain current after exposure, $I_{DS,air}$ is the drain current before exposure and ΔI_{ref} is the current increase of the control device exposed in air.

Table S2. Comparison of Key Parameters of electrical toluene sensors using OCS as active layers.

Sensing Material	Sensor Type	Response definition †	Detect Limit	Sensitivity response	Reference
This work **P3HT:SSIL**	**Chemiresistor (2 terminal)**	**$\Delta R/R_0$**	**30 ppm**	**-5% at 1500 ppm**	
P3HT	Chemiresistor (2 terminal)	ΔG/G	400 ppm	-1.43% per 1ppm	[3]
PDDT-*ran*-PMT	Chemiresistor (2 terminal)	ΔG/G	200 ppm	-19.6% per 1ppm	[3]
PHT-*b*-PS	Chemiresistor (2	ΔG/G	10 ppm	20.5% per	[3]

	terminal)			1ppm	
PHT-*b*-PMA	Chemiresistor (2 terminal)	ΔG/G	200 ppm	14.6% per 1ppm	[3]
P3HT	Chemiresistor (2 terminal)	$\Delta I_{DS}/I_{DS}$	50 ppm	$5x10^{-6}$ per ppm	[4]
P3HT	Transistor (3 terminal)	$\Delta I_{DS}/I_{DS}$	280 ppm	$5x10^{-7}$ per ppm	[4]
PAH-2	Transistor (3 terminal)	$\Delta I/I_0$	0.1 p_a/p_0‡	-0.8	[9]
PAH-3	Transistor (3 terminal)	$\Delta I/I_0$	0.1 p_a/p_0‡	5.7	[9]
PAH-4	Transistor (3 terminal)	$\Delta I/I_0$	0.1 p_a/p_0‡	0.6	[9]
PAH-7	Transistor (3 terminal)	$\Delta I/I_0$	0.1 p_a/p_0‡	-0.4	[9]

† Response definition as given in source: ΔG/G = change in normalised conductance change, $\Delta I_{DS}/I_{DS}$ and $\Delta I/I_0$ = normalised source drain current response.

‡ Concentration 0.1 p_a/p_0 as given in source, approximated to 100 000 ppm using ppmv=vapor pressure of analyte (p_a) / atmospheric pressure (p_0) $x10^6$

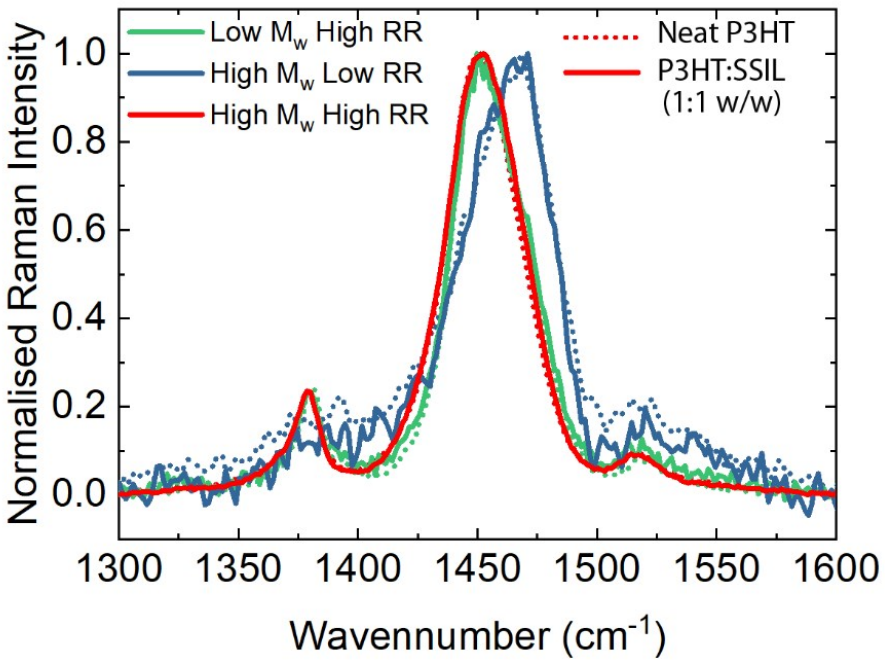

Fig. S8. Steady state Raman spectroscopy with 488 nm excitation of P3HT neat and P3HT:SSIL 1:1 for low M_w high RR (green), high M_w low RR (blue) and high M_w high RR (red) P3HT blends

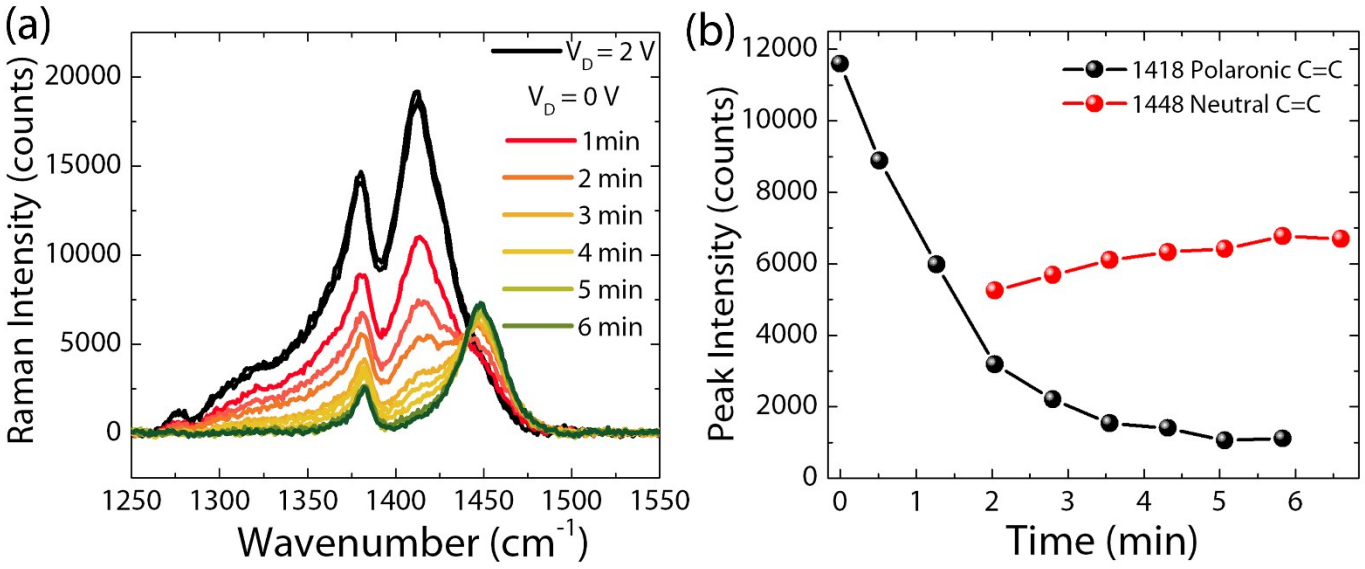

Fig. S9. Reversibility of FRDS. a) in situ Raman spectra and b) the peak intensity of polaronic signal (1418 cm-1) returns to the neutral peak (1448 cm-1) showing the slow reversible process when the applied voltage is lowered from -2 V to 0 V and Raman signature returns to the neutral peak position after several minutes.

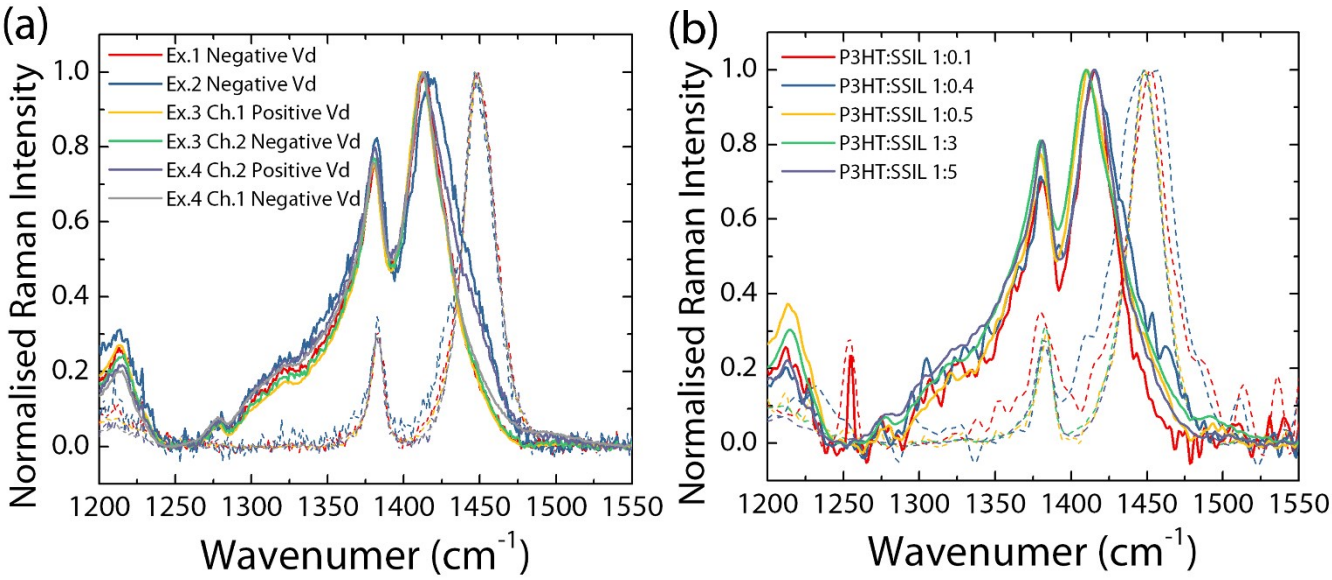

Fig. S10. Reproducibility of FRDS a) repeat conditions of P3HT:SSIL 1:1 blend over six experimental conditions and b) varying blend ratios from P3HT:SSIL 1:0.1 to 1:5. Neural P3HT signal (1415 cm-1) is seen at 0V (dashed line) and under an applied voltage of VD = ±1.5 V (solid line) shows the polaronic peak signals at 1448 cm-1.

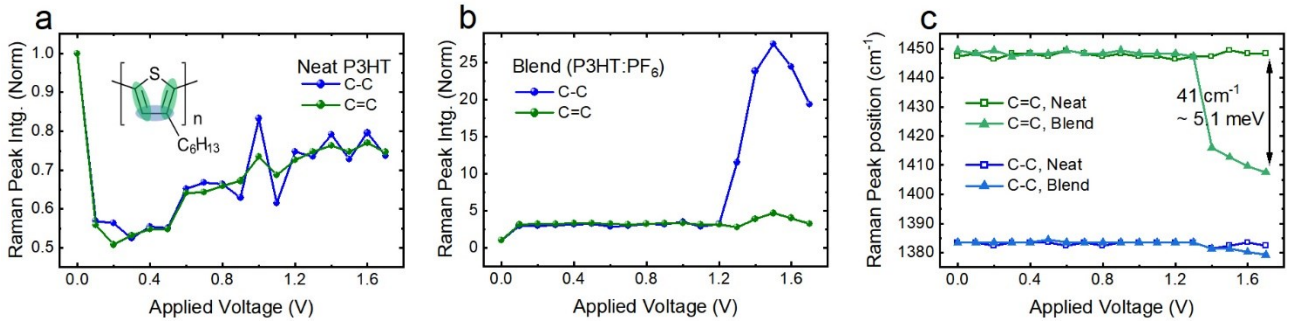

Fig. S11. Integrated total peak area (C=C and C-C intraing modes) for a) neat P3HT and b) P3HT:SSIL and c) peak position (C=C and C-C intraing modes) for neat and blend as a function of applied voltage. The values are extracted from field-dependent Raman spectroscopy (FDRS) shown in Figure 5.

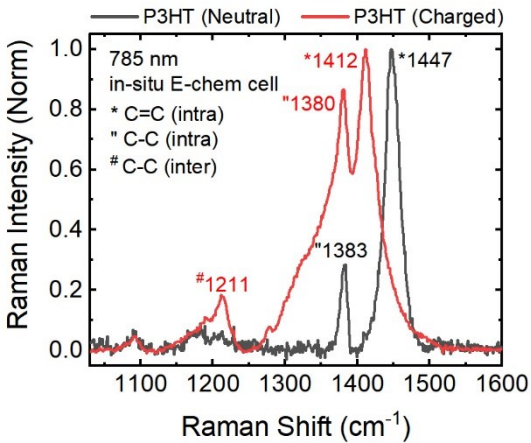

Fig. S12. Baseline corrected and normalized Raman spectra for neutral and charged (hole-polaronic) P3HT acquired at 785 nm (non-resonant to ground-state absorption, resonant to polaronic absorption) in-situ electrochemical cell. The charged spectra correspond to hole polaron density (nd) in the P3HT film ~ 1×1021 cm-3 (based on our previous published report[20]).

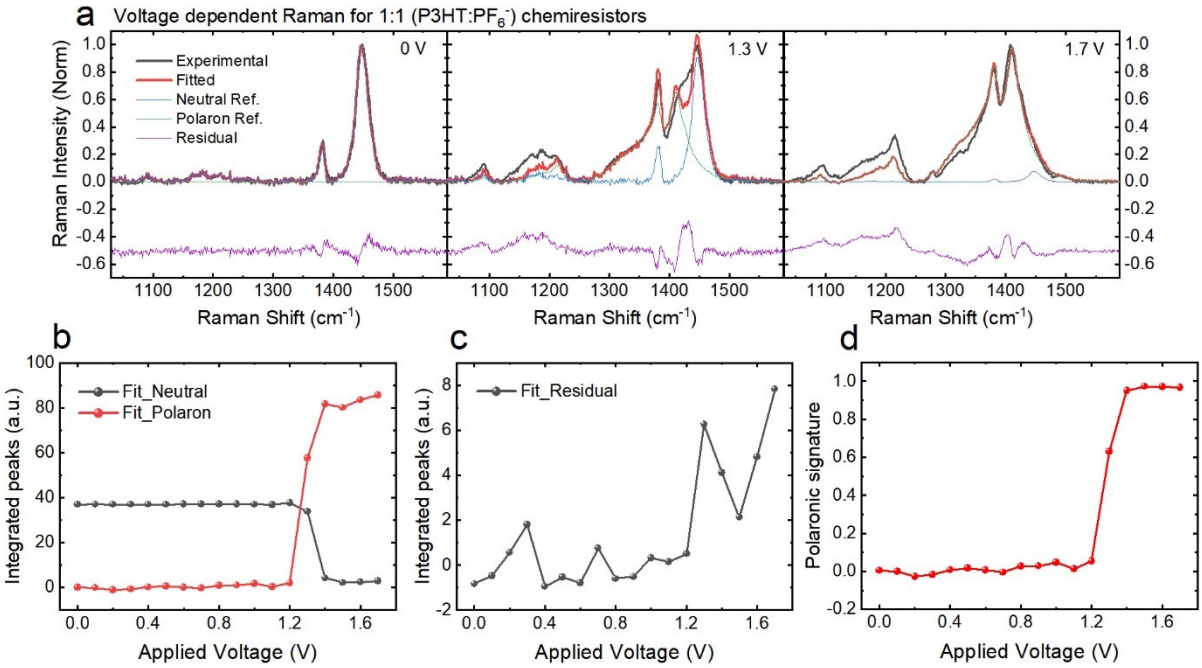

Fig. S13. Fits to the experimentally obtained Raman spectra of P3HT:SSIL blends at different applied voltages (in-situ chemiresistor) via reference neutral and polaronic spectra of P3HT (also experimentally obtained as shown in Figure S6). b) Integrated intensity of the fitted neutral and polaronic spectra across range of applied voltages (extracted from a). c) Fitting residuals. d) Polaronic signature against applied voltages across the chemiresistor, obtained via $I_P/I_P + I_n$; where I_P is integrated polaronic spectra and I_n is the integrated neutral spectra after fitting the experimental data (see a).

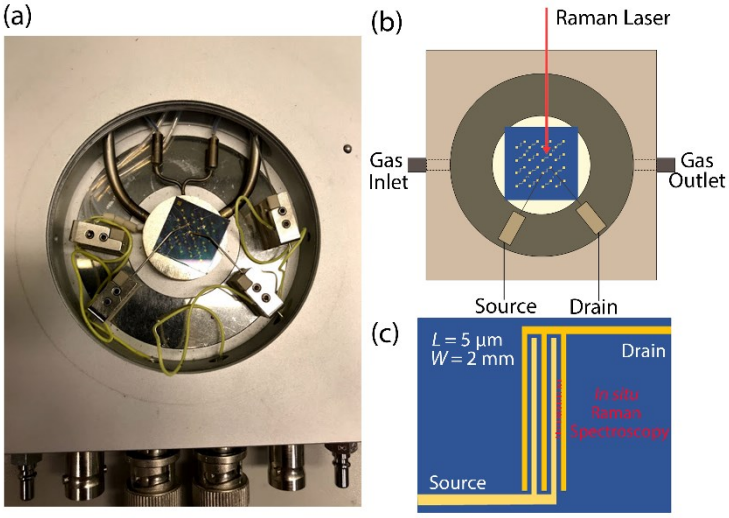

Figure S14. a) Image of chemiresistor in *in situ* measurement chamber, schematic diagram showing b) the set up used for FDRS and *in situ* gas sensing where voltage is applied by a power source meter, the gas flow runs across the chamber and the Raman is probed through viewing window and c) *in situ* Raman spectroscopy on a 5 µm showing the 20 scans taken down the channel while under controlled electrical atmosphere conditions.

References

1 V. Dua, S. P. Surwade, S. Ammu, S. R. Agnihotra, S. Jain, K. E. Roberts, S. Park, R. S. Ruoff and S. K. Manohar, *Angew. Chemie - Int. Ed.*, 2010, **49**, 2154–2157.

2 T. P. Mokoena, Z. P. Tshabalala, K. T. Hillie, H. C. Swart and D. E. Motaung, *Appl. Surf. Sci.*, 2020, **525**, 146002.

3 B. Li, G. Sauvé, M. C. Iovu, M. Jeffries-El, R. Zhang, J. Cooper, S. Santhanam, L. Schultz, J. C. Revelli, A. G. Kusne, T. Kowalewski, J. L. Snyder, L. E. Weiss, G. K. Redder, R. D. McCullough and D. N. Lambeth, *Nano Lett.*, 2006, **6**, 1598–1602.

4 B. Li and D. N. Lambeth, *Nano Lett.*, 2008, **8**, 3564–3567.

5 J. Lu, D. Liu, J. Zhou, Y. Chu, Y. Chen, X. Wu and J. Huang, *Adv. Funct. Mater.*, , DOI:10.1002/adfm.201700018.

6 B. Peng, S. Huang, Z. Zhou and P. K. L. Chan, *Adv. Funct. Mater.*, 2017, **27**, 1–8.

7 L. Li, P. Gao, M. Baumgarten, K. Müllen, N. Lu, H. Fuchs and L. Chi, *Adv. Mater.*, 2013, **25**, 3419–3425.

8 H. Li, J. Dailey, T. Kale, K. Besar, K. Koehler and H. E. Katz, *ACS Appl. Mater. Interfaces*, 2017, **9**, 20501–20507.

9 A. Bayn, X. Feng, K. Müllen and H. Haick, *ACS Appl. Mater. Interfaces*, 2013, **5**, 3431–3440.